Original Article

Asian Pacific Journal of Tropical Biomedicine

Ethanol extract of *Abelmoschus manihot* suppresses endoplasmic reticulum stress in contrast−induced nephropathy

Xin Lin, Xin Lu, Yun−He Zhao, Yi−Bei Wang, Ru−Ge Niu, Xiao−Hu Chen✉

Department of Cardiology, Affiliated Hospital of Nanjing University of Chinese Medicine, Jiangsu Province Hospital of Chinese Medicine, Nanjing, Jiangsu 210004, China

ABSTRACT

Objective: To explore the efficacy and potential mechanisms of the ethanol extract of *Abelmoschus manihot* (L.) Medic in contrast-induced nephropathy (CIN).

Methods: CIN rat models and human renal proximal tubular cells (HK-2) with iopromide-induced injury were employed to mimic CIN conditions. The effect of *Abelmoschus manihot* extract on the rat models and HK-2 cells was evaluated. In rat models, kidney function, histology, oxidative stress and apoptosis were determined. In HK-2 cells, cell viability, apoptosis, mitochondrial membrane potential, and endoplasmic reticulum stress were assessed.

Results: *Abelmoschus manihot* extract significantly improved structural and functional impairments in the kidneys of CIN rats. Additionally, the extract effectively mitigated the decline in cellular viability and reduced iopromide-induced oxidative stress and lipid peroxidation. Mechanistic investigations revealed that *Abelmoschus manihot* extract prominently attenuated acute endoplasmic reticulum stress-mediated apoptosis by downregulating GRP78 and CHOP protein levels.

Conclusions: *Abelmoschus manihot* extract can be used as a promising therapeutic and preventive agent in the treatment of CIN.

KEYWORDS: Contrast-induced nephropathy; *Abelmoschus manihot* extract; ER stress; Apoptosis; GRP78; CHOP

1. Introduction

Contrast-induced nephropathy (CIN) is a form of acute kidney injury that may arise after administration of contrast agents, particularly iodine-based ones, in medical imaging procedures like computed tomography or angiography[1,2]. Characterized by a swift deterioration in renal function[3], CIN affects up to 50%

of patients with chronic kidney disease undergoing coronary angiography[4,5]. Strategies aimed at mitigating the risk of CIN encompass prehydration through intravenous fluids, utilization of low-osmolarity contrast agents, employing antioxidants such as *N*-acetylcysteine, and fenoldopam administration[6]. It is important to acknowledge that the efficacy of these preventive measures varies based on patient profiles and clinical contexts. Despite considerable research efforts, conclusive evidence regarding the optimal preventive strategies for CIN remains elusive. Extensive literature is marked by conflicting findings, impeding the formulation of unequivocal guidelines[7,8]. The identification of individuals at high risk of CIN (such as those with preexisting renal conditions, diabetes, advanced age, or comorbidities) coupled with the exploration of alternative imaging modalities or techniques minimizing contrast usage, can significantly attenuate the probability of CIN development[9]. It is important to note that the most recent

---

Significance

Our previous clinical investigations have corroborated the benefits of *Abelmoschus manihot* in patients with contrast-induced nephropathy. However, the precise mechanisms remain unclear. The current study found that *Abelmoschus manihot* reduced iopromide exposure-induced kidney injury by inhibiting endoplasmic reticulum stress both *in vivo* and *in vitro*.

✉To whom correspondence may be addressed. E-mail: yfy0007@njucm.edu.cn

guidelines refrain from recommending a specific treatment regimen due to the nebulous nature of its underlying mechanism.

Certain Chinese herbs have demonstrated efficacy in ameliorating symptoms linked to edema, hematuria, and kidney disease[10], and among these botanicals is *Abelmoschus manihot* (*A. manihot*) (L.) Medicus. This plant is distributed across Eastern Europe and temperate and subtropical regions of Asia, and its flowers are employed in traditional Chinese medicine to treat chronic kidney disease[11]. The Jiahua tablet (the trade name of *A. manihot*), an indigenous product developed by our hospital, has secured regulatory approval for clinical application in the management of chronic glomerulonephritis. Previous clinical investigations conducted by our team have corroborated the beneficial effects of the Jiahua tablet in patients with CIN[12,13], although its precise mechanism remains unclear. A randomized controlled trial conducted by an external research team reported that intervention with *A. manihot* in individuals with primary glomerular disease over a week significantly diminished urinary protein content and protected kidney function, surpassing the effects of losartan potassium[14]. Furthermore, it exhibited efficacy in reducing urinary protein in cases of nephrotic syndrome. Importantly, *A. manihot* demonstrated favorable results in the treatment of diabetic nephropathy with minimal adverse effects[15,16]. *In vitro* experiments also revealed that the ethanol extract of *A. manihot* mitigated iopromide-induced apoptosis in renal tubular epithelial cells (HK-2 cells)[17]. Considering the above beneficial effects of *A. manihot*, the current study aimed to investigate the effect of *A. manihot* on iopromide-induced HK-2 cells and a CIN rat model.

2. Materials and methods

2.1. Preparation of ethanol extract of A. manihot

The flowers of *A. manihot* were completely submerged in 75% ethanol and subsequently extracted at 90 ℃. The solution was collected after 1 h, filtered, and evaporated under vacuum conditions at 60 ℃, yielding dry extract powder. This powder was then aseptically stored at −20 ℃. Before use, the extract was dissolved in sterile water, and ultrasonic treatment was performed.

2.2. High−performance liquid chromatography (HPLC) analysis

The composition of *A. manihot* extract was characterized using an HPLC system (Waters e2695, Waters Corporation) equipped with a C18 chromatographic column (250 mm × 4.6 mm, 5 μm). To create a reference stock solution, appropriate quantities of hyperoside (lot no. C10180684), myricetin (lot no. C10079514), quercetin (lot no. C10298448), rutin (lot no. C10275778, all from Macklin, Shanghai,

China), and isoquercitrin (lot no. P25J9F65872, Yuanye, Shanghai, China) were weighed and prepared at a concentration of 1 mg/mL in a methanol aqueous solution. Various volumes of the reference solution were mixed and diluted to generate a mixed reference solution containing these five components. According to HPLC analysis, the primary components of the prepared *A. manihot* extract were identified.

2.3. Animals and grouping

Adult male Sprague Dawley rats (180-200 g, 7-8 weeks, Qinglongshan Animal Breeding Center, Nanjing, China) were acclimatized for one week before being randomly assigned to four groups (*n*=8 per group): (i) control, (ii) model, (iii) low *A. manihot* extract (1.5 g/kg body weight), and (iv) high *A. manihot* extract (3.0 g/kg body weight)[18]. As described previously[19,20], the rats received injections of the prostaglandin synthesis inhibitor indomethacin (10 mg/kg, *i.v.*) and the nitric oxide inhibitor NG-nitro-*L*-arginine methyl ester (*L*-NAME, 10 mg/kg, *i.v.*). Contrast media iopromide (3 g iodine/kg, *i.v.*) was administered after 15 min. All rats received drugs according to their respective groups for one week before modeling. The control group received gastric perfusion with the corresponding vehicle on each occasion. Body weights were recorded, and urine was collected every 24 h in metabolic cages to monitor urine output.

2.4. Sample collection

Orbital plexus blood was collected and subsequently centrifuged to obtain serum, which was then stored at −80 ℃. Following weighing and euthanasia using CO_2 (30% of the chamber volume/min), all kidneys were collected and kidney index was calculated (index = kidney weight/body weight). A portion of kidney tissues was frozen in liquid nitrogen and stored at −80 ℃. The remaining kidney tissues were fixed in 4% paraformaldehyde and embedded in paraffin for histological examination and immunohistochemistry (IHC) analysis.

2.5. Biochemical index detection

Commercially available kits (Jiancheng Bioengineering Institute, Nanjing, China) were used to determine serum creatinine (SCr), malondialdehyde (MDA), and glutathione (GSH) levels. The renal tissue homogenate was prepared, and the supernatant was collected. These biochemical indices were measured following the respective manufacturer's instructions.

2.6. Hematoxylin−eosin (H&E) staining

Renal tissue specimens were fixed with 4% paraformaldehyde, dehydrated with graded alcohol, and subsequently embedded in

paraffin. After dewaxing, 5 μm tissue sections underwent H&E staining (Sangon Biotech, Shanghai, China). Images were captured under an inverted microscope (Nikon, Tokyo, Japan).

2.7. IHC staining

Renal tissue sections were dewaxed in xylene for 15 min, rehydrated with graded ethanol, and double-distilled water. The slides were immersed at room temperature for 15 min in a 3% hydrogen peroxide solution. Antigen retrieval was achieved by incubating the slides in citrate buffer solution (pH 6.0) and heating them in a microwave oven 3 times for 8 min. The slides were then blocked for 1 h with 10% bovine serum (ExCell Bio, Shanghai, China) and incubated with primary antibodies overnight in a moist box at 4℃. Following three washes with phosphate-buffered saline (PBS) with Tween, the tissue sections were incubated with an anti-rabbit secondary antibody labeled with biotin and streptavidin labeled with horseradish peroxidase. Antibody information is provided in Supplementary Table 1. DAB solution (Bioss, Beijing, China) was added, followed by counterstaining with hematoxylin for 3 min. Images were captured under an inverted microscope (Nikon, Tokyo, Japan).

2.8. TUNEL assay

Dewaxed slices were permeabilized using 0.3% Triton X-100 in PBS for 30 min and washed three times with PBS. TUNEL staining solution (50 μL, Sangon Biotech, Shanghai, China) was incubated with sections in the dark for 1 h at 37℃. DAPI staining solution was added, then the sections were incubated in the dark for 10 min and washed with PBS. Images were captured using a fluorescence microscope (Nikon Ni-U, DS-Qi2, Japan).

2.9. Cell culture

HK-2 cells (Procell, Wuhan, China) were cultured in DMEM/F-12 (Gibco, Thermo Fisher Scientific) supplemented with 10% fetal bovine serum (ExCell Bio, Shanghai, China) at 37℃ with 5% CO_2. Cells were passaged upon reaching 80%-90% confluence.

2.10. 3−(4,5−dimethylthiazol−2−yl)−2,5−diphenyltetrazolium bromide (MTT) assay

The MTT assay was utilized to determine the viability of HK-2 cells. Approximately 5 000 cells were seeded in 96-well plates and incubated for 24 h. Cells were then treated with different concentrations of iopromide (30, 70, 100, 120, 150, and 180 mg I/mL) or *A. manihot* extract (0.1, 0.2, 0.4, 0.8, 1, 2, 4, and 8 mg/mL)[17] for 24 h. Cells in each well were incubated in serum-free medium and MTT reagent (10×, Sangon Biotech, Shanghai, China) for 3 h, followed by

the replacement with 200 μL DMSO. A microplate reader was used to measure the absorbance at 490 nm (Bio Tek, Santa Clara, CA, USA).

2.11. Annexin V−FITC/PI double staining assay

HK-2 cells were seeded in 6-well culture plates and grown to 90% confluence. The cells were treated with different concentrations of *A. manihot* extract for 24 h. Cells were collected, washed with cold PBS, and stained with Annexin V-FITC and PI (Procell, Wuhan, China) for 15 min in the dark at room temperature. The fluorescent signal was detected using flow cytometry (Becton Dickinson, Franklin Lakes, NJ, USA).

2.12. Immunofluorescence staining

HK-2 cells were seeded in confocal dishes (Nest, Wuxi, China), washed with PBS three times for 5 min each, fixed with 4% paraformaldehyde for 15 min at 4℃, and then treated with 0.3% Triton X-100 for 15 min for permeabilization. After a 5% BSA blocking step for 1 h, cells were incubated overnight at 4℃ with a primary antibody. After three PBS washes, cells were incubated for 90 min with CoraLite488-conjugated Goat Anti-Rabbit IgG at room temperature and then washed more than three times. DAPI staining solution was added, and the samples were incubated in the dark for 5 min. A Zeiss confocal laser microscope (ZEISS LSM 700, Oberkochen, Battenfurt, Germany) was used for localization analysis.

2.13. Measurement of mitochondrial membrane potential

The JC-1 assay (Beyotime, Jiangsu, China) was used to investigate mitochondrial membrane potential. HK-2 cells were seeded in a 6-well culture plate ($2×10^5$ cells/well). After treatment, the cells were collected in a brown Eppendorf tube and incubated in 1 mL JC-1 staining buffer at 37℃ for 20 min. Following incubation, the supernatant was removed, and cells were washed twice with JC-1 staining buffer (1×). Images were captured using a fluorescence microscope (Nikon Ni-U, DS-Qi2, Japan).

2.14. Measurement of reactive oxygen species (ROS)

2′,7′-Dichlorofluorescein (DCF) and dihydroethidium (DHE) probes (Solarbio, Beijing, China) were used to assess ROS levels in cells, as described in a previous report[21]. Images were captured using a fluorescence microscope (Nikon Ni-U, DS-Qi2, Japan).

2.15. Western blot analysis

HK-2 cells were lysed in RIPA buffer (Beyotime, Jiangsu, China) supplemented with a 2% protease and phosphatase inhibitor

cocktail for 20 min on ice. The samples were centrifuged at 4℃ for 10 min after sonication, supernatants were collected, and total protein concentration was determined with a BCA protein assay kit (Beyotime, Jiangsu, China). Equal amounts of protein (20 μg) were separated using 8%, 10%, or 12% sodium-dodecyl sulfate-polyacrylamide gel electrophoresis and transferred to polyvinylidene difluoride membranes (Millipore, Billerica, MA, USA). The membranes were blocked in 5% non-fat milk for 2 h at room temperature. Subsequently, they were incubated with primary antibodies overnight at 4℃. After washing, the membranes were incubated with HRP-conjugated anti-rabbit or anti-mouse IgG for 1 h at room temperature. The blots were developed using a chemiluminescence substrate (Thermo Fisher Scientific), and images were acquired with a Tanon 5200 chemiluminescent imaging system (Tanon, Shanghai, China). Image Lab software was used for quantitative analysis. Antibody information is provided in Supplementary Table 1.

2.16. Statistical analysis

Statistical analysis was conducted using SPSS software (IBM, Armonk, NY, USA). All data are presented as mean ± standard deviation. To compare two groups, unpaired, two-tailed student's *t*-tests were conducted. Analysis of variance (ANOVA) and Dunnett's test were employed for multiple groups. $P<0.05$ was considered statistically significant.

2.17. Ethical statement

All animal experiments complied with the ARRIVE guidelines and were carried out in accordance with the National Institutes of Health guide for the care and use of Laboratory animals. The Ethics Review Committee of Nanjing Tech University approved the animal experiments (No. LL-20220325-03).

3. Results

3.1. A. manihot alleviates the renal injury in CIN rats

The HPLC analysis revealed that hyperoside, isoquercitrin, myricetin, quercetin, and rutin were the main components of the prepared *A. manihot* extract (Figure 1). The simplified animal protocol is presented in Figure 2A. For kidney index (Figure 2B) and body weight (Figure 2C), there were slight differences among experiment groups. The urine output of rats in the model group was decreased compared with the control group at three time points, and the rats treated with *A. manihot* extract exhibited higher urine output than the model group at 24 and 72-h intervals, although the difference was not significant (Figure 2D). Nevertheless, *A. manihot* extract effectively suppressed the increase of SCr in CIN rats (Figure 2E). H&E staining showed that the model group exhibited vacuolar degeneration, necrotic or exfoliated cell debris in the lumen of the renal tubules, and thickened interstitium, compared with the control group. In contrast, *A. manihot* extract at a low dose alleviated tissue damage, and inflammatory infiltration persisted, which was largely normalized in the high-dose treatment group (Figure 2F).

3.2. A. manihot attenuates oxidative damage both in vivo and in vitro

The MDA in the tissues of the model group was significantly increased (Figure 3A), which was significantly reduced by both doses of *A. manihot* extract. Moreover, the GSH content was
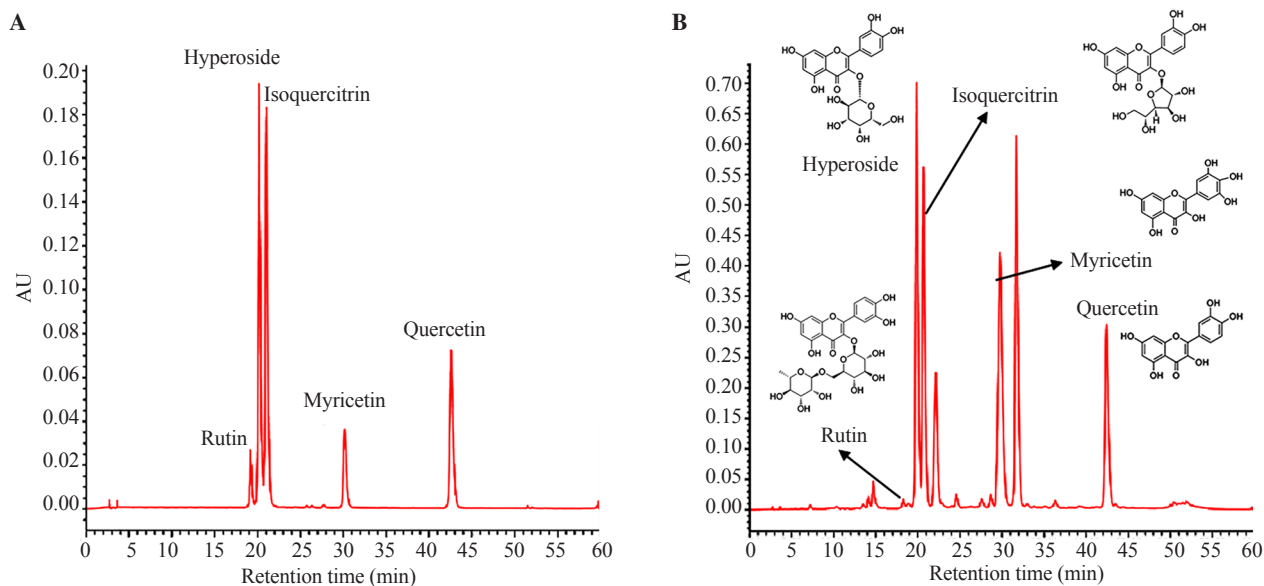

Figure 1. Fingerprint analysis of *Abelmoschus manihot* by HPLC. (A) Standard; (B) *Abelmoschus manihot.*

markedly decreased in the model group, which was reversed by *A. manihot* extract (Figure 3B). In addition, IHC analysis showed that the positive rates of 4-HNE and 8-OHdG in the model group were significantly enhanced, whereas the group treated with a high dose of *A. manihot* extract displayed decreased contents of 4-HNE and 8-OHdG in the tissue (Figure 3C). *N*-acetyl-cysteine (NAC), a typical ROS inhibitor, was used as a control substance. The results of DCF and DHE probes in HK2 cells reflected the production and accumulation of ROS in the model group. *A. manihot* extract significantly abolished the overproduction of ROS, consistent with the trend induced by NAC (Figure 3D).

3.3. A. manihot hinders the apoptosis in kidney tissues and HK−2 cells

TUNEL staining revealed that apoptotic cells in the kidney tissue of the model group increased markedly. However, *A. manihot* extract effectively reduced apoptosis (Figure 4A-B). Western blot analysis demonstrated that the extract significantly decreased the levels of cleaved caspase-3 and cleaved PARP proteins (Figure 4C-E). Consistently, IHC staining revealed that *A. manihot* extract diminished the expression of cleaved caspase-3 and cleaved PARP (Figure 4F).

In HK-2 cells, cell viability was decreased by iopromide in a concentration-dependent manner (Figure 5A). In contrast, *A. manihot* extract (0.1-8 mg/mL) did not affect cell viability (Figure 5B). *A. manihot* extract (0.6 mg/mL) could ameliorate the iopromide-induced decrease in cell viability in HK-2 cells (Figure 5C). In subsequent experiments, cells were treated with 100 mg I/mL iopromide and 0.4 or 0.6 mg/mL *A. manihot* extract. Flow cytometry analysis exhibited that both extract and NAC could reduce iopromide-induced apoptosis (Figure 5D). Western blot results showed that the protein levels of cleaved caspase-3 and cleaved PARP in cells were markedly decreased by treatment with *A. manihot* extract (Figure 5E-G). Early stages of apoptosis were assessed in terms of mitochondrial membrane potential. Compared with the control group, JC-1 monomers were significantly increased, and aggregates were decreased in the model group, while the extract and
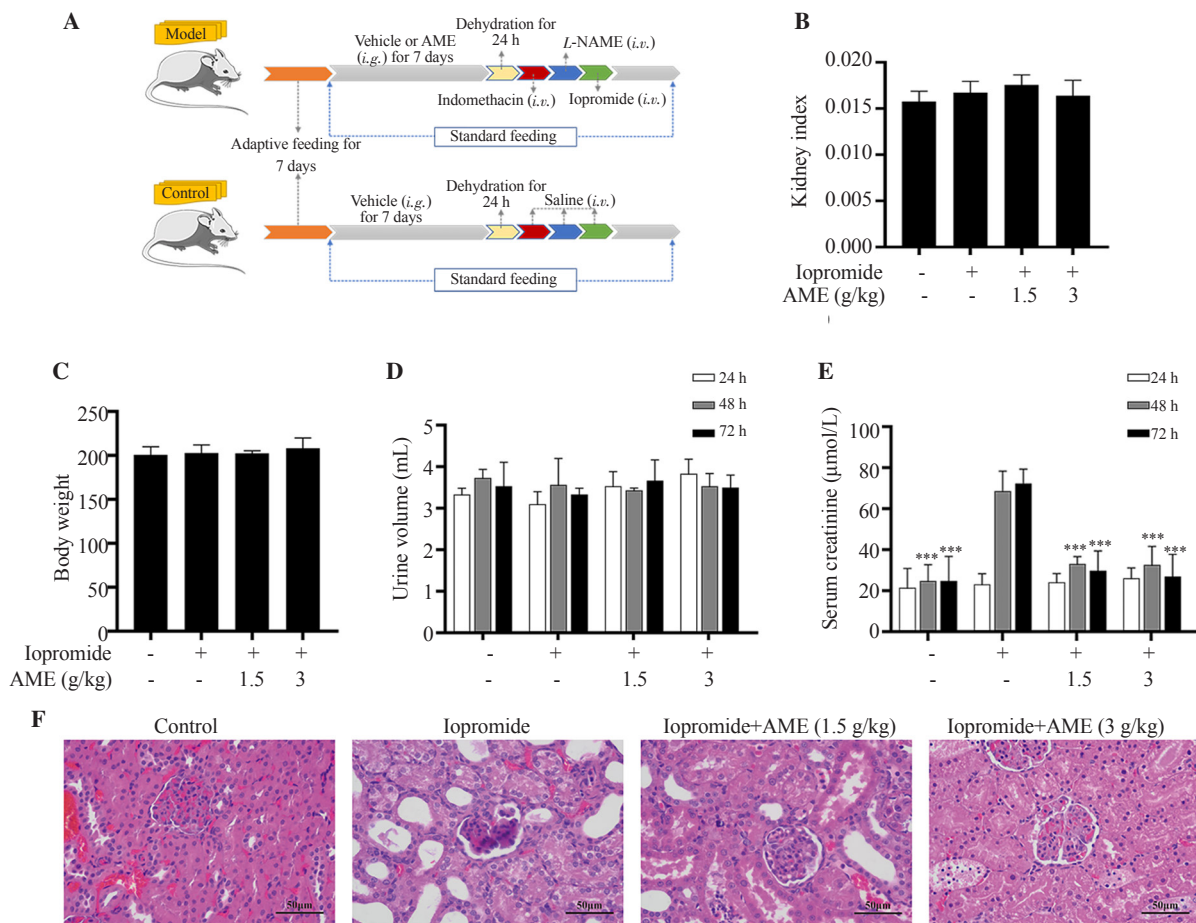
Figure 2. *Abelmoschus manihot* extract alleviates renal injury in rats with contrast-induced nephropathy. (A) The simplified animal protocol. The effects of the extract on the (B) kidney index, (C) rat body weight, (D) urine volume, and (E) serum creatinine. Kidney index = organ weight/rat body weight. ***$P<0.001$ *vs.* the model group. (F) H&E staining exhibits pathological changes in kidney tissues, including vacuolar degeneration or exfoliated fragments within the renal tubule lumen, interstitial thickness, and inflammatory infiltration (400×). AME: *Abelmoschus manihot* extract; *L*-NAME: NG-nitro-*L*-arginine methyl ester.
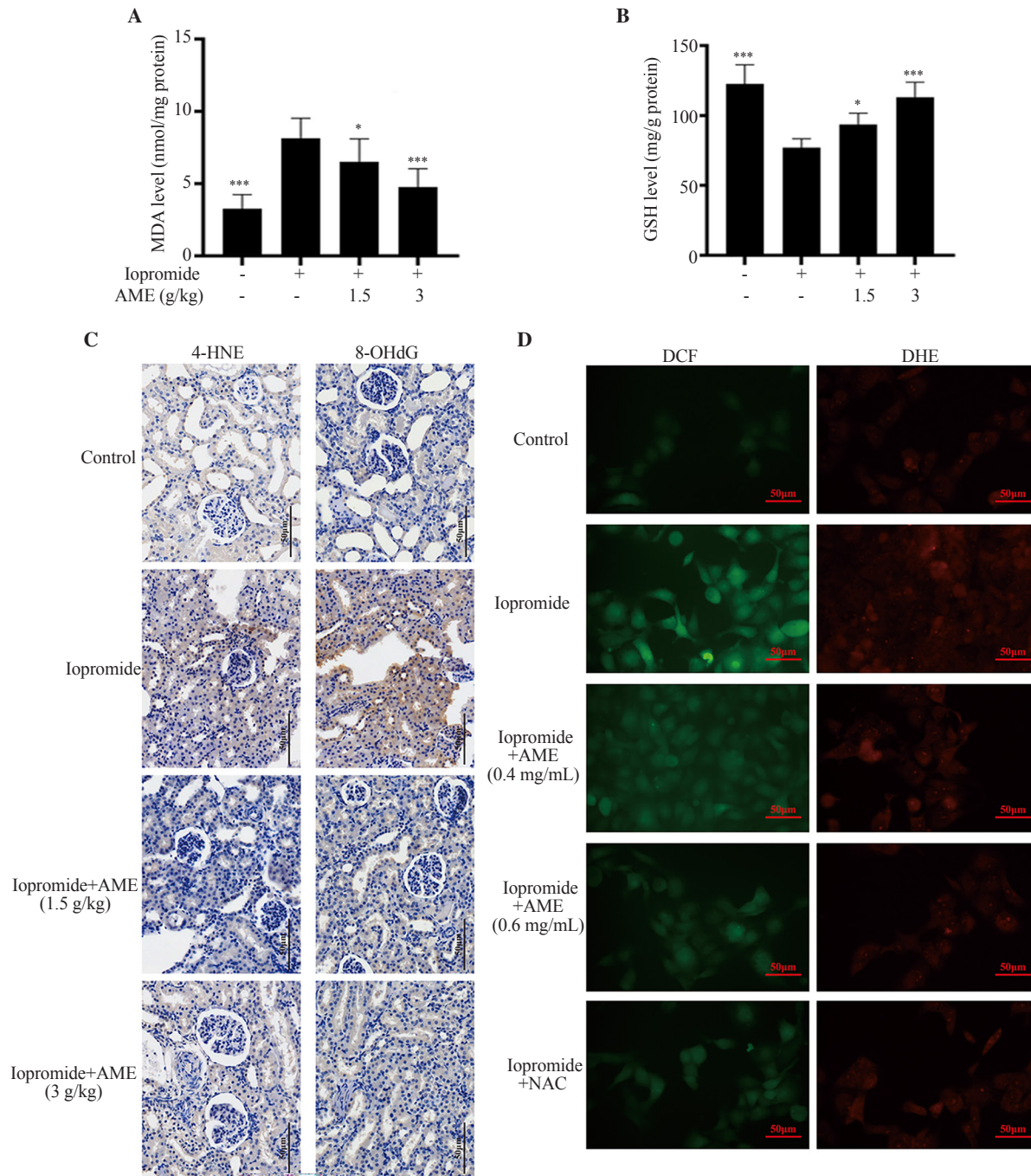
Figure 3. *Abelmoschus manihot* extract attenuates oxidative damage both *in vivo* and *in vitro*. (A) The levels of MDA and (B) GSH in the kidney tissues. (C) Representative IHC images of 4-HNE and 8-OHdG in the kidney tissues (400×). (D) DCF (green) and DHE probes (red) indicate the ROS levels (400×). $^{*}P<0.05$, $^{***}P<0.001$ *vs.* the model group. NAC: *N*-acetyl-cysteine.

NAC treatment significantly reduced JC-1 monomers, indicating that *A. manihot* extract effectively reversed the decreased mitochondrial membrane potential (Figure 5H-I).

3.4. A. manihot reduces acute endoplasmic reticulum (ER) stress

Western blot analysis revealed that compared with the control group, the protein levels of CHOP and GRP78 in the model group showed an upward trend. Whereas, *A. manihot* extract significantly decreased the levels of CHOP and GRP78 proteins in tissues (Figure 6A-C). According to IHC staining, the positive signals of CHOP and GRP78 in the model group were higher than those in the control group, which were significantly decreased by *A. manihot* extract (Figure 6D). Similar findings were obtained in cell experiments, where CHOP and GRP78 proteins were significantly decreased in
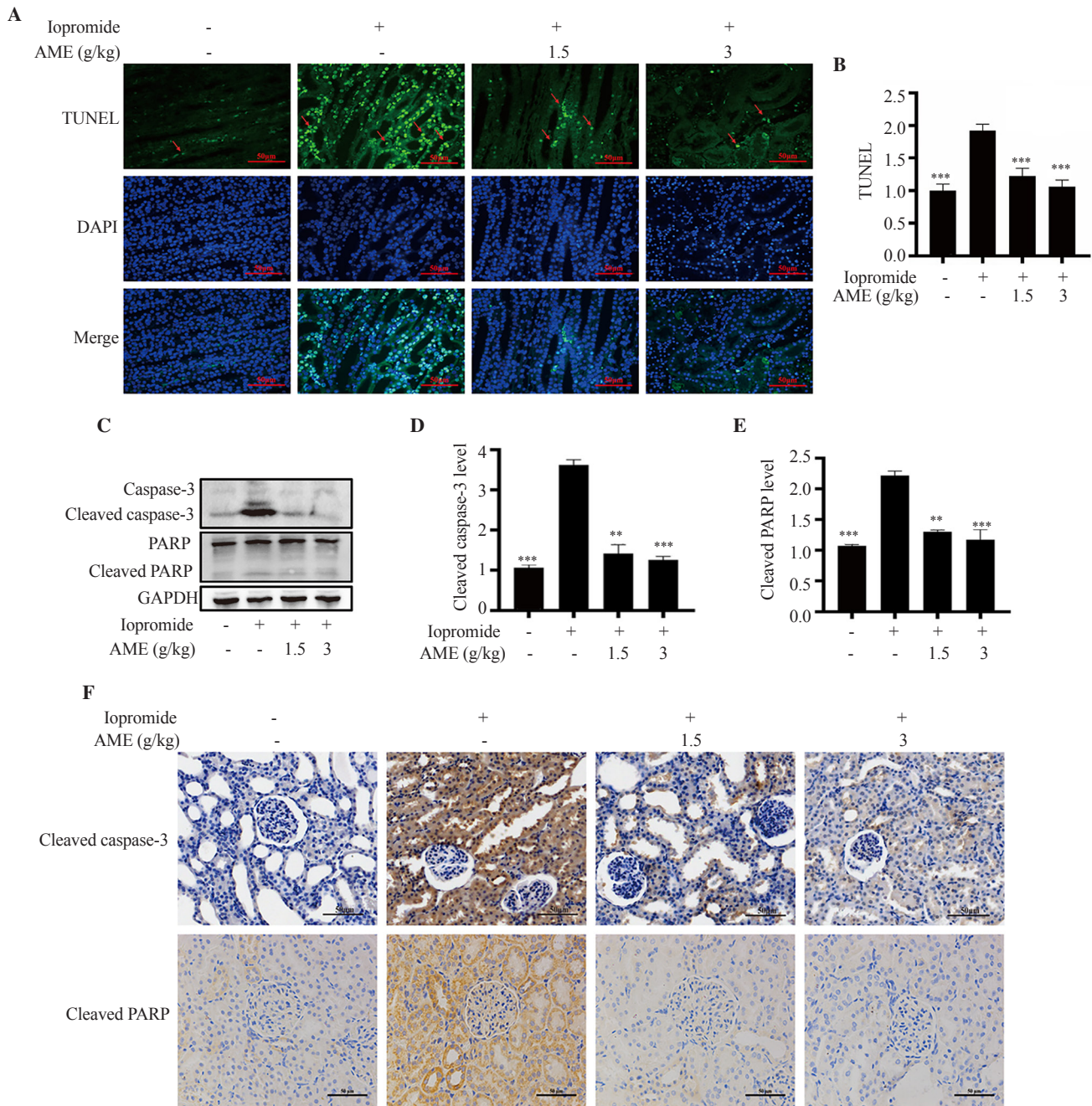
Figure 4. *Abelmoschus manihot* extract reduces apoptosis in kidney tissues. (A) The effect of the extract on apoptosis was determined by TUNEL staining (400×). (B) Semi-quantitative results of TUNEL staining. (C) The cleaved caspase-3 and cleaved PARP protein levels were examined by Western blot. (D and E) Semi-quantitative results of Western blot. (F) Representative IHC images of cleaved caspase-3 and cleaved PARP in the kidney tissues (400×). $^{**}P<0.01$, $^{***}P<0.001$ *vs.* the model group.

HK-2 cells treated with *A. manihot* extract and NAC, respectively (Figure 6E-G). Furthermore, CHOP expression in the nucleus and cytoplasm of HK-2 cells was identified using immunofluorescence. The CHOP level in the model group was higher compared to the control group, whereas *A. manihot* extract (0.6 mg/mL) reduced the positive area (Figure 6H). Thus, the extract attenuated acute ER stress in both CIN rats and iopromide-induced HK-2 cells.

4. Discussion

Medical imaging has identified CIN as a prominent contributor to iatrogenic kidney injury[22]. This investigation has validated the involvement of ER stress-mediated apoptosis in CIN. Remarkably, *A. manihot* extract exhibits the capacity to ameliorate CIN by abating ER stress-mediated apoptosis. A previous study also suggests that ER stress mediates the mechanism of the *Aspergillus* plant extract against cardiovascular endothelial damage[23]. Notably, patients
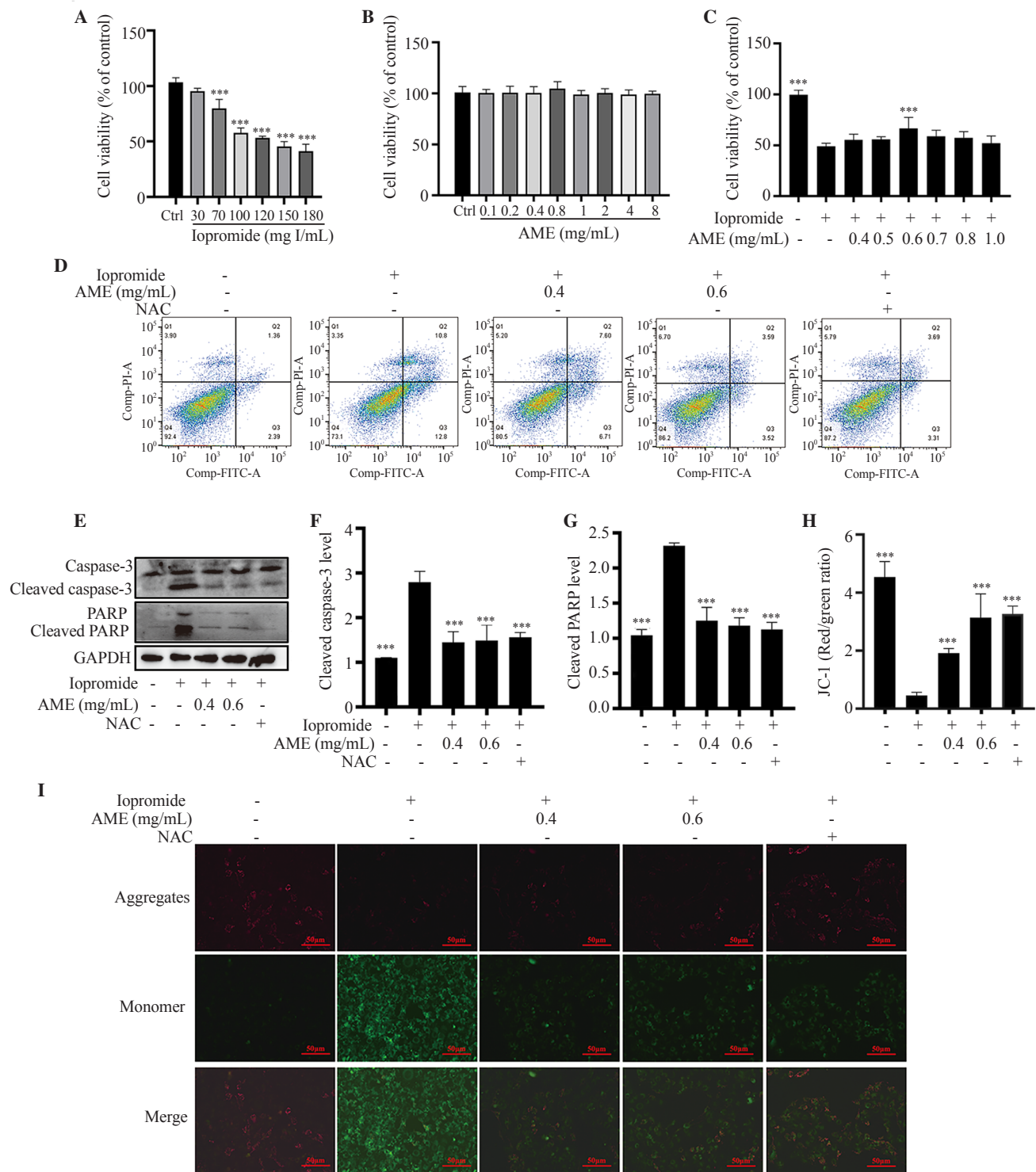
Figure 5. *Abelmoschus manihot* extract decreases apoptosis in HK-2 cells. The effect of (A) iopromide, (B) *Abelmoschus manihot* extract, and (C) iopromide+ *Abelmoschus manihot* extract on HK-2 cell viability. (D) HK-2 cell apoptosis was determined by flow cytometry. (E) Caspase-3 and PARP protein expression were examined by Western blot analysis. (F and G) Semi-quantitative results of Western blot. (H) Semi-quantitative results of JC-1 assay. (I) JC-1 probe was utilized to detect mitochondrial membrane potential (200×). $^{***}P<0.001$ *vs.* the model group.

afflicted with cardiovascular and cerebrovascular conditions, such as acute myocardial infarction and stroke, display heightened susceptibility to CIN[24]. Thus, early intensive intervention becomes imperative for potentially high-risk CIN patients. A comprehensive assessment of CIN risk is necessary for patients undergoing contrast medium injections[25]. Given the current evidence and guideline recommendations, specific therapeutic measures for CIN remain elusive, underscoring the significance of prevention as a primary approach to reducing CIN incidence. The pursuit of novel strategies for both the prevention and treatment of CIN persists as a formidable
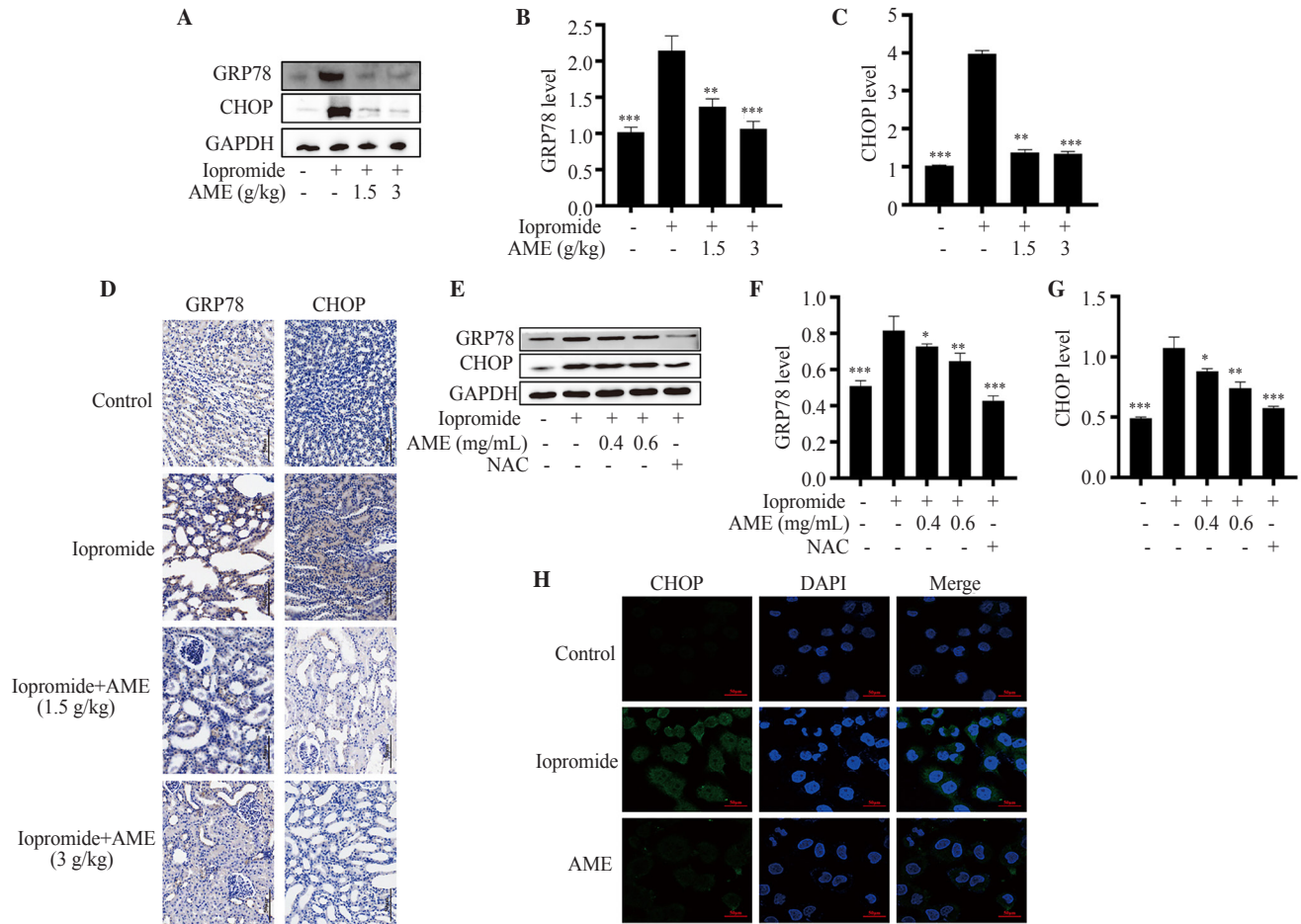
Figure 6. *Abelmoschus manihot* extract reduces acute ER stress. (A) The effect of the extract on the protein levels of GRP78 and CHOP in the kidney tissues was examined by Western blot. (B and C) Semi-quantitative results of Western blot. (D) Representative IHC images of GRP78 and CHOP protein expression in the kidney tissues (400×). (E-G) Western blot analysis of CHOP and GRP78 protein expression in HK-2 cells and their semi-quantitative results. (H) Immunofluorescence analysis of CHOP protein levels (630×). *P<0.05, **P<0.01, ***P<0.001 *vs.* the model group.

challenge.

Mechanistically, contrast agents accumulate within the kidney and are subsequently reabsorbed by renal tubules, impeding efficient glomerular filtration and elongating the duration of contrast agent exposure to renal tubular epithelial cells. Prolonged exposure intensifies tubular ischemia and hypoxia, culminating in pronounced cellular damage or apoptosis[26]. Our data corroborate the induction of apoptosis in HK-2 cells and rat kidney tissue by iopromide, an iodine-based contrast agent, affirming the successful establishment of the model.

Previous research has emphasized that contrast agent-triggered renal ischemia and hypoxia elevate renal oxidative stress[22]. ROS partake in cell signal transduction processes *via* the renal tubular transport system, orchestrating key messengers and pivotal transcription factors. Renal parenchymal hypoxia is exacerbated through ROS-mediated direct damage to renal tubules and vascular endothelium, often aggravating hypoxia through endothelial dysfunction and imbalanced tubular transport[27]. Consequently, pertinent experiments were carried out to examine the role of

A. manihot extract in mitigating oxidative damage within the pathological mechanism of CIN. Our results substantiate its potential to curtail contrast-induced oxidative stress and renal lipid peroxidation, an exacerbating factor for oxidative damage.

Emerging evidence has consistently situated acute ER stress as a precursor to apoptosis[28]. The maintenance of ER homeostasis, protein folding, assembly facilitation, and misfolded protein elimination is overseen by GRP78[29]. Under normal circumstances, CHOP maintains low expression levels. However, under ER stress conditions, it dissociates from ER transmembrane proteins, activating the expression of apoptosis-associated proteins[30,31]. Our investigation highlights the ability of *A. manihot* extract to suppress acute ER stress in kidney tissue exposed to iopromide. Nevertheless, there are limitations in this study. Given the presence of several compounds in *A. manihot* extract, it would be of interest to define the optimal composition ratio or screen out the most critical medicinal ingredients in future research.

Collectively, our findings indicate that *A. manihot* extract can significantly mitigate renal pathological damage and oxidative stress

in CIN rats. Additionally, *A. manihot* extract reduced apoptosis and ER stress in both *in vivo* and *in vitro* experiments. This study provides an initial insight into its mechanism in alleviating CIN-related damage.

Conflict of interest statement

The authors declare that they have no conflict of interest.

Acknowledgments

Funding

Data availability statement

The data supporting the findings of this study are available from the corresponding authors upon request.

Authors᾽ contributions

XC contributed to the conceptualization, experiment design and manuscript revision. X. Lin, X. Lu, YZ and YW contributed to the investigation and methods. RN and X. Lin contributed to the formal analysis and writing draft. The final version has been reviewed and approved by all authors.

References

[1] Pistolesi V, Regolisti G, Morabito S, Gandolfini I, Corrado S, Piotti G, et al. Contrast medium induced acute kidney injury: A narrative review. *J Nephrol* 2018; **31**(6): 797-812.

[2] Barrett T, Khwaja A, Carmona C, Martinez Y, Nicholas H, Rogers G, et al. Acute kidney injury: Prevention, detection, and management. Summary of updated NICE guidance for adults receiving iodine-based contrast media. *Clin Radiol* 2021; **76**(3): 193-199.

[3] Chandiramani R, Cao D, Nicolas J, Mehran R. Contrast-induced acute kidney injury. *Cardiovasc Interv Ther* 2020; **35**(3): 209-217.

[4] Nabi Z, Anjum N, Rashid RM, Zahideen ZU. Contrast induced nephropathy in high risk patients - Myth or reality. *J Ayub Med Coll Abbottabad* 2021; **33**(4): 568-571.

[5] Azzalini L, Kalra S. Contrast-induced acute kidney injury-definitions, epidemiology, and implications. *Interv Cardiol Clin* 2020; **9**(3): 299-309.

[6] Liu S, Shan XG, Zhang XJ. The place of hydration using intravenous fluid in patients at risk of developing contrast-associated nephropathy. *Br J Hosp Med (Lond)* 2020; **81**(9): 1-7.

[7] Timal RJ, Kooiman J, Sijpkens YWJ, de Vries JPM, Verberk-Jonkers I, Brulez HFH, et al. Effect of no prehydration *vs* sodium bicarbonate prehydration prior to contrast-enhanced computed tomography in the prevention of postcontrast acute kidney injury in adults with chronic kidney disease: The Kompas randomized clinical trial. *JAMA Intern Med* 2020; **180**(4): 533-541.

[8] Zaki HA, Bashir K, Iftikhar H, Alhatemi M, Elmoheen A. Evaluating the effectiveness of pretreatment with intravenous fluid in reducing the risk of developing contrast-induced nephropathy: A systematic review and meta-analysis. *Cureus* 2022; **14**(5): e24825.

[9] Rudnick MR, Leonberg-Yoo AK, Litt HI, Cohen RM, Hilton S, Reese PP. The controversy of contrast-induced nephropathy with intravenous contrast: What is the risk? *Am J Kidney Dis* 2020; **75**(1): 105-113.

[10]Ma S, Zhao M, Chang M, Shi X, Shi Y, Zhang Y. Effects and mechanisms of Chinese herbal medicine on IgA nephropathy. *Phytomedicine* 2023; **117**. doi: 10.1016/j.phymed.2023.154913.

[11]Luan F, Wu Q, Yang Y, Lv H, Liu D, Gan Z, et al. Traditional uses, chemical constituents, biological properties, clinical settings, and toxicities of *Abelmoschus manihot* L.: A comprehensive review. *Front Pharmacol* 2020; **11**. doi: 10.3389/fphar.2020.01068.

[12]Wu Q, Lin X, Miao X, Liu F. Effect of Jiahua tablet on renal injury index in patients with contrast nephropathy after coronary angiography or interventional therapy. *J Nanjing Univ Tradit Chin Med* 2020; **36**(2): 189-192.

[13]Lin X, Wang Y, Miao X, Gao K, Wu Q. Clinical study of Jiahua tablet in the prevention and treatment of contrast nephropathy in patients with coronary intervention. *J Modern Integr Tradit Chin West Med* 2020; **29**(35): 3882-3885.

[14]Zhang L, Li P, Xing CY, Zhao JY, He YN, Wang JQ, et al. Efficacy and safety of *Abelmoschus manihot* for primary glomerular disease: A prospective, multicenter randomized controlled clinical trial. *Am J Kidney Dis* 2014; **64**(1): 57-65.

[15]Li N, Tang H, Wu L, Ge H, Wang Y, Yu H, et al. Chemical constituents, clinical efficacy and molecular mechanisms of the ethanol extract of *Abelmoschus manihot* flowers in treatment of kidney diseases. *Phytother Res* 2021; **35**(1): 198-206.

[16]Zhao J, Tostivint I, Xu L, Huang J, Gambotti L, Boffa JJ, et al. Efficacy of combined *Abelmoschus manihot* and irbesartan for reduction of albuminuria in patients with type 2 diabetes and diabetic kidney disease: A multicenter randomized double-blind parallel controlled clinical trial.

Diabetes Care 2022; **45**(7): e113e115.

[17]Xu Z, Qian L, Niu R, Wang Y, Yang Y, Liu C, et al. Mechanism of *Abelmoschus manihot* L. in the treatment of contrast-induced nephropathy on the basis of network pharmacology analysis. *Front Nephrol* 2022; **2**. doi: 10.3389/fneph.2022.834513.

[18]Li W, He W, Xia P, Sun W, Shi M, Zhou Y, et al. Total extracts of *Abelmoschus manihot* L. attenuates adriamycin-induced renal tubule injury *via* suppression of ROS-ERK1/2-Mediated NLRP3 inflammasome activation. *Front Pharmacol* 2019; **10**. doi: 10.3389/fphar.2019.00567.

[19]Sugiura T, Hirasawa Y, Toyoshi T, Matsumura Y. Effects of agmatine on contrast-induced nephropathy in rats and rabbits. *Biol Pharm Bull* 2020; **43**(10): 1556-1561.

[20]Iordache AM, Buga AM, Albulescu D, Vasile RC, Mitrut R, Georgiadis G, et al. Phosphodiesterase-5 inhibitors ameliorate structural kidney damage in a rat model of contrast-induced nephropathy. *Food Chem Toxicol* 2020; **143**. doi: 10.1016/j.fct.2020.111535.

[21]Ren C, Bao X, Lu X, Du W, Wang X, Wei J, et al. Complanatoside A targeting NOX4 blocks renal fibrosis in diabetic mice by suppressing NLRP3 inflammasome activation and autophagy. *Phytomedicine* 2022; **104**. doi: 10.1016/j.phymed.2022.154310.

[22]Zhang F, Lu Z, Wang F. Advances in the pathogenesis and prevention of contrast-induced nephropathy. *Life Sci* 2020; **259**. doi: 10.1016/j.lfs.2020.118379.

[23]Sireesh D, Suganya N, Chatterjee S, Ramkumar KM. *Gymnema montanum* improves endothelial function *via* inhibition of endoplasmic reticulum stress by activating Nrf2 signaling. *Asian Pac J Trop Biomed* 2020; **10**(8): 379-386.

[24]Kusirisin P, Chattipakorn SC, Chattipakorn N. Contrast-induced nephropathy and oxidative stress: Mechanistic insights for better interventional approaches. *J Transl Med* 2020; **18**(1): 400.

[25]Mamoulakis C, Tsarouhas K, Fragkiadoulaki I, Heretis I, Wilks MF, Spandidos DA, et al. Contrast-induced nephropathy: Basic concepts, pathophysiological implications and prevention strategies. *Pharmacol Ther* 2017; **180**: 99-112.

[26]Vlachopanos G, Schizas D, Hasemaki N, Georgalis A. Pathophysiology of contrast-induced acute kidney injury (CIAKI). *Curr Pharm Des* 2019; **25**(44): 4642-4647.

[27]Andreucci M, Faga T, Pisani A, Sabbatini M, Michael A. Acute kidney injury by radiographic contrast media: Pathogenesis and prevention. *Biomed Res Int* 2014; **2014**. doi: 10.1155/2014/362725.

[28]Shu S, Wang H, Zhu J, Liu Z, Yang D, Wu W, et al. Reciprocal regulation between ER stress and autophagy in renal tubular fibrosis and apoptosis. *Cell Death Dis* 2021; **12**(11): 1016.

[29]Teng J, Liu M, Su Y, Li K, Sui N, Wang S, et al. Down-regulation of GRP78 alleviates lipopolysaccharide-induced acute kidney injury. *Int Urol Nephrol* 2018; **50**(11): 2099-2107.

[30]Zhong Y, Jin C, Han J, Zhu J, Liu Q, Sun D, et al. Inhibition of ER stress attenuates kidney injury and apoptosis induced by 3-MCPD *via* regulating mitochondrial fission/fusion and Ca^{2+} homeostasis. *Cell Biol Toxicol* 2021; **37**(5): 795-809.

[31]Yan M, Shu S, Guo C, Tang C, Dong Z. Endoplasmic reticulum stress in ischemic and nephrotoxic acute kidney injury. *Ann Med* 2018; **50**(5): 381-390.

Publisher's note

The Publisher of the *Journal* remains neutral with regard to jurisdictional claims in published maps and institutional affiliations.

Edited by Liang Q, Tan BJ